Laser Chem. 1987, Vol. 7, pp. 141–176
Photocopying permitted by license only

Printed in the United Kingdom

Intra- and Intermode Vibrational Energy Flow in CH_3F Excited by Irradiation with an Intense CO_2 Laser: A Non-Linear Vibrational Relaxation

HIDEAKI NAKANE† and SOJI TSUCHIYA

Department of Pure and Applied Sciences, College of Arts and Sciences, The University of Tokyo, Komaba, Meguro-ku, Tokyo 153, Japan

The vibrational relaxation mechanism of CH_3F whose ν_3 mode is excited by a transversely excited atmospheric (TEA)CO_2 laser-pulse has been discussed on the basis of observation of the laser-induced fluorescence (LIF) of the ν_3 overtones and of the C–H stretching modes and kinetic analyses. The time-evolved LIF in the 3-μm region was found to be dependent significantly on the laser fluence; at a low fluence ($<0.01\,J\,cm^{-2}$), the emission intensity increased almost exponentially with a rate similar to the one determined in the experiment with a Q-switched laser, while at a higher fluence ($>0.1\,J\,cm^{-2}$) the emission rose much faster to form a peak which decayed quickly before a second broad peak appeared. In the wavelength-resolved fluorescence measurement, it was found that the kinetics of population in the ν_4 level were similar to those in the $3\nu_3$ level, while those in the ν_1, $2\nu_5$, $\nu_2+\nu_5$ and $2\nu_2$ levels behaved in a way different from those in the ν_4 level. These observations lead to the conclusion that the laser energy poured into the ν_3 mode flows to the ν_4 level directly through $3\nu_3$ as well as by the successive inter- and intramode V–V energy transfers, i.e., $\nu_3 \rightarrow \nu_6 \rightarrow \nu_2$, $\nu_5 \rightarrow 2(\nu_2, \nu_5) \rightarrow \nu_1 \rightarrow \nu_4$. A model calculation of the relaxation kinetics, including the direct V–V energy transfer between two $3\nu_3$ and ν_4 levels, could reproduce the 3-μm emission data. Another significant finding is a non-exponential depopulation in the $2\nu_3$ level, the ν_4, ν_1 and other vibrational levels in the 3-μm region in the final stage of the relaxation. The deactivation rate is larger for a higher level and is a decreasing function of time and is much larger than the V–T/R energy transfer rate determined in the

† Present address: National Institute for Environmental Studies, PO Tsukuba-gakuen, Ibaraki 305, Japan.

experiment of weak laser excitation. This may be attributed primarily to the successive intermode V–V energy transfers from the $3\nu_3$ to the ν_4, ν_1, $2\nu_5$, . . . levels which lie between the $2\nu_3$ and $3\nu_3$ levels. This process may be repeated if the intramode V–V energy transfer from the $2\nu_3$ to the $3\nu_3$ level occurs. The deactivation mechanism found in this experiment is called 'catastrophic cyclic path' which is effective until the relative population distribution in relevant levels between $2\nu_3$ and $3\nu_3$ becomes that in equilibrium at the translational temperature of the CH_3F gas.

KEY WORDS: Vibrational relaxation; IR laser-induced fluorescence; vibrational energy transfer; CH_3F, vibrational relaxation of.

INTRODUCTION

In dealing with the mechanism of vibrational energy flow in polyatomic molecules whose specific vibrational mode is excited by laser irradiation, it has become the general consensus that the intramode vibration-to-vibration (V–V) energy transfer dominates the intermode V–V so that a local vibrational quasiequilibrium distribution is attained within the laser-pumped vibrational mode prior to establishment of the steady-state distribution among all modes, and that in the final stage of the relaxation, the vibration-to-translation/rotation (V–T/R) energy transfer occurs from modes having low fundamental frequencies. The former studies on the vibrational relaxation of a number of small polyatomic molecules support this mechanism and are reviewed in detail by Flynn[1].

Of the polyatomic molecules, CH_3F has been investigated the most intensively for its vibrational relaxation. Since the ν_3 C–F stretching mode of CH_3F has the lowest vibrational frequency resonant to the CO_2 laser line and the V–T/R relaxation is relatively slow, a large part of the energy pumped into the ν_3 mode by the CO_2 laser irradiation is stored within various vibrational modes for a relatively long period. This implies that under a quasiequilibrium condition, a population distribution with a high vibrational temperature is realized in each mode, and CH_3F could thus be one of the polyatomic molecules which are adequate for more detailed investigation of their intra- and intermode energy transfer mechanism on the basis of observations of laser-induced fluorescence (LIF).

According to the aforementioned general principle of vibrational relaxation, the CH_3F molecules which have absorbed CO_2 laser photons in the ν_3 mode transfer their energies to the ν_4 mode through the following pathway (*see* Figure 1):

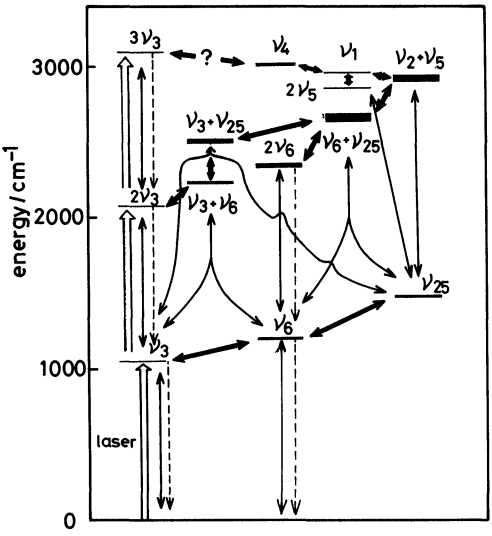

Figure 1 Vibrational energy level diagram of CH_3F in which each level represents its degeneracy, and energy transfer reaction is shown by an arrow. In the present model, ν_1, $2\nu_5$ and $\nu_2 + \nu_5$ are represented by ν_{125}. $\longleftrightarrow$: intramode V–V; $\Longleftrightarrow$: intermode V–V; :$\longleftrightarrow$: V–T/R energy transfer.

$$\nu_3 \rightarrow \nu_6 \rightarrow \nu_2,\ \nu_5 \rightarrow 2\nu_2,\ 2\nu_5 \rightarrow \nu_1 \rightarrow \nu_4 \tag{1}$$

This mechanism was proved by Sheorey and Flynn[2] and Apkarian and Weitz[3] in the LIF measurement of CH_3F excited by a Q-switched CO_2 laser. Contrary to this, another pathway, which includes the intramode V–V ladder climbing within the ν_3 mode and the near-resonant intermode V–V energy transfer between $3\nu_3$ and ν_4:

$$\nu_3 \rightarrow 2\nu_3 \rightarrow 3\nu_3 \rightarrow \nu_4 \rightarrow \nu_1 \rightarrow 2\nu_2,\ \nu_2 + \nu_5,\ 2\nu_5 \tag{2}$$

has been proposed based on high-resolution spectroscopic data; this indicates that a number of rotational levels of the $3\nu_3$ state are strongly Coriolis coupled with those of the ν_4 state[4]. The main reason for preference of the pathway in Eqn (1) rather than that in Eqn (2) is that the populations in the bending overtones, $2\nu_2$ and $2\nu_5$, are much larger than those in the $3\nu_3$ level and, moreover, that bending overtones and C—H stretching modes are coupled with each other by Fermi as well as Coriolis interaction[5,6]. In the pathway of Eqn (1), the population rate in the ν_4 level should not depend on the average number of CO_2 laser

photons absorbed per CH_3F molecule. Nevertheless, Kneba and Wolfrum[7] found that the rise rate of the 3-μm emission induced by irradiation of CH_3F with the 9.6-μm P(20) line of a TEA CO_2 laser was much larger than that predicted by Eqn (1). A similar phenomenon which could not be explained by Eqn (1) was also reported by Sheorey and Flynn[2]. When CH_3F was irradiated by the focused beam of a Q-switched CO_2 laser pulse, an initial fast rise of the ν_1, ν_4 (C—H stretching) emission occurred, which was followed by a partial decay and later by a second slower rise to a broad maximum. As a possible interpretation of this finding, it was suggested that a rapid increase of the population in the ν_1, $\nu_4 + \nu_3$ level caused the initial fast rise of the 3-μm emission.

The present authors proposed the pathway in Eqn (2) as a mechanism to explain the aforementioned phenomenon found in the 3-μm emission induced by irradiation of CH_3F with a TEA CO_2 laser[8]. However, Forber *et al.*[9] opted for Eqn (1) as a dominant energy flow mechanism on the basis of the measurement of the vibrational temperature for each mode of $^{13}CH_3F$ excited by a TEA CO_2 laser. More recently, Apkarian *et al.*[10] carried out a model calculation of coupled rate equations which were formulated based on Eqn (1) as well as Eqn (2) to conclude that the direct V–V transfer from $3\nu_3$ to ν_1/ν_4 could not occur even under a strong laser excitation condition, since the vibrational heat capacity of the ν_1, ν_4, $2\nu_2$, $\nu_2 + \nu_5$, $2\nu_5$ levels was too large to fill them from $3\nu_3$.

If the observed increase of the population rate in the ν_1, ν_4 levels of CH_3F molecules whose ν_3 mode is excited by a strong CO_2 laser is attributed to the existence of the pathway in Eqn (2) as well as Eqn (1), the intermode V–V energy transfer from the $3\nu_3$ to the ν_4 level must be extraordinarily efficient. According to the established view[1] of the collision probability of V–V energy transfer rates, its rate may not be large unless both the energy non-resonance, which must be transferred to/from translation/rotation, and the change in the number of vibrational quanta are minimized. Therefore, it would be of fundamental importance to clarify the mechanism of the intermode energy flow in CH_3F molecules whose specific mode is excited by a strong CO_2 laser.

In this paper, we report the measurements of the wavelength-resolved infrared (IR) fluorescence from CH_3F whose ν_3 mode is excited by irradiation with a TEA CO_2 laser and the kinetic analysis of the relaxation process. The main purpose of this study is to test

whether the kinetics of the population in each vibrational level is dependent or not on an initial amount of the laser energy which is poured into the ν_3 mode of CH_3F and to seek a more general vibrational energy flow mechanism which is applicable irrespective of the extent of laser irradiation.

EXPERIMENTAL

The ν_3 mode of CH_3F in a gas cell was excited by irradiation with the 9.4-μm P(20) line of a TEA CO_2 laser (Lumonics, TE-102-2). The laser pulse energy was adjusted in the range of 0.7–0.01 J by placing an appropriate number of polyethylene films (0.01 mm in thickness) in the pathway of the laser beam as an attenuator. The laser energy and the pulse shape were measured by a calorimeter (Gentec, Ed-500) and by a photon-drag detector (Rofin, 7400), respectively. The pulse was composed of a spike of 200-nm FWHM and a tail of 1.5 μs duration when the laser medium was a mixture of $He : CO_2 : N_2 = 3 : 1 : 0.4$ and the pulse repetition frequency was 2.5 Hz. The cross-section of the laser beam was reduced to the size of 9.5×6.5 mm by use of a ZnSe condenser lens, so that the laser fluence was increased up to 1 J cm^{-2}.

The laser intensity was not completely homogeneous throughout the cross-section. In fact, the fluence distribution across the beam cross-section was determined by probing energy of the laser beam which passed through a pin-hole of 1 mm inner diameter by a pyroelectric energy meter. The result of this measurement indicates that it is a good approximation to assume the above size of the cross-section for homogeneous intensity of the laser beam.

Two types of gas cell were employed. The first one was designed according to the proposal of Manuccia and Frankel[11], and was employed for measurement of the dispersed LIF spectrum. The second was one for observing a time-evolved IR fluorescence at a fixed wavelength. Both systems were composed of a Pyrex glass cell (10 cm i.d. and 30 cm in length) which includes two mirror systems: one for multiple reflection of the incident laser beam and the other for collection of the induced IR fluorescence. The latter mirror system was of the Welsh type[12]. In the first arrangement of the cell, five plane mirrors were placed inside the cell as a pentagonal column whose internal surfaces enabled the incident laser beam to traverse a long

distance when the incident direction of the beam was slightly tilted from one perpendicular to the column axis. In this experiment, the incident laser beam reflected on the internal mirrors 24 times, its pathlength being about 1.5 m; at the end of the beam's traverse the laser intensity was attenuated to about one-half of the original value. Sice this attenuation was unfavorable for quantitative discussion of the fluorescence data, a second arrangement of the mirror system was employed; the laser beam was reflected only three times by two parallel plane mirrors placed 12 cm apart from each other, so that the attenuation of the laser intensity was less than 10%. The LIF collected by the Welsh mirror system was taken to a monochromator ($f = 3.4$) with a 4-μm blazed grating of 300 groove mm^{-1} or to band pass filters for 3 and 5-μm regions before illuminating an InSb photovoltaic detector (Fujitsu, IV200). The signal was initially treated by a current preamplifier (PAR, 181) whose frequency response was d.c. to 0.67 MHz (−3 dB), and this output was amplified by an amplifier (Brookdeal, 9454) with a bandwidth of 0.1 Hz–3 MHz (−3 dB). The final signal was digitized and accumulated by a data processor (Iwasaki, SM 1300). Normally, 1024 or 2048 data were averaged to improve the *S/N* ratio. The time response function of the detector system was determined to be about 3 μs by use of a GaAs IR emission diode which was pulsed by an electric square wave. Calibration of the sensitivity of the monochromator, including the detecting system, was made by a spectral measurement of the radiation from a homemade black body furnace. The discharge noise of the TEA CO_2 laser was employed as a trigger pulse for timing the signal processing system; the time between the trigger and the CO_2 laser pulse was determined to be 1.5–0.5 μs by monitoring the laser pulse by the photon-drag detector. The fluctuation of this delay time was disregarded because of the relatively long response time of the detector. Special attention was paid to reducing the discharge noise of the TEA CO_2 laser which interfered significantly with the signal processing. The entire laser apparatus was covered by copper plates of 0.3 mm in thickness, and the LIF measurement system, including the monochromator, the detector and the current preamplifier, was also shielded by copper plates.

The sample gas of CH_3F was a commercial gas (PCR) with a nominal purity of 97–98%, and was employed after repeated solidification at liquid N_2 temperature. According to the mass spectroscopic analysis, the impurity content was less than 0.4%. The pressure of the sample

gas in the cell was measured with a capacitance manometer (MKS Baratron, 210).

The average number of CO_2 laser photons which were absorbed by one CH_3F molecule was determined by the absorption measurement; the attenuation of the laser beam through traversing a cell of 1 m in length containing CH_3F was determined by the energy measurement of the laser pulse.

RESULTS AND DISCUSSION

Undispersed LIF at 3μm

The observed temporal behavior of the 3-μm emission from CH_3F whose ν_3 mode is excited by irradiation with a TEA CO_2 laser, 9.4-μm P(20) line, is shown in Figure 2 as a function of the laser energy fluence. The data taken at a low fluence and reproduced in Figure 2(a) shows that the emission rises almost exponentially to a plateau, although a large discharge noise of the laser makes it difficult to trace the initial rise of the emission accurately. Disregarding the noise, it is seen that the rise rate is in the same order of magnitude as the one reported on the excitation by a Q-switched CO_2 laser (cf. Figure 6(b) of Ref. 2). In contrast to this, as shown in Figure 2(b), increasing the fluence of the laser, the emission rises much faster to form a peak which is followed by a second broad peak. This observation is analogous to that found by Sheorey and Flynn[2] under focused irradiation with a Q-switched CO_2 laser (cf. Figure 6(a) of Ref. 2). In the data of Figure 2(c) which has been observed at the highest fluence of this experiment, the emission forms a clear peak in the initial stage, while the second broad peak in Figure 2(b) changes to a shoulder of the initial peak.

The results shown in Figure 2 imply that we may not apply the energy flow mechanism of Eqn (1) to interpret the observed dependence of the 3-μm emission of the laser fluence. According to the mechanism of Eqn (1), the vibrational relaxation proceeds towards a quasiequilibrium state, in which the population distribution in each mode is of the Boltzmann type. Therefore, populations in respective levels except those of the laser-pumped mode may not exceed the magnitudes defined by the quasiequilibrium condition. For example, populations in the ν_1 and ν_4 levels grow after the pulsed excitation of the ν_3 mode and approach the steady-state values with a rate defined by

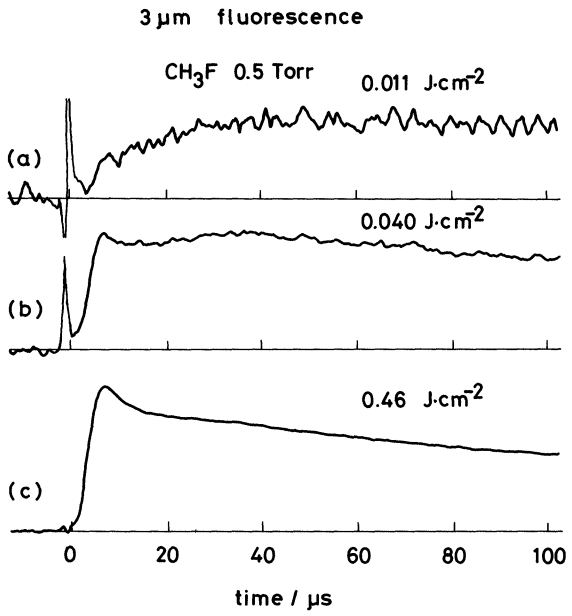

Figure 2 Time-evolved LIF taken through the 3-μm bandpass filter as a function of the energy fluence of the TEA CO_2 laser at 0.5 Torr of CH_3F pressure. A spike signal at $t = 0$ is due to the discharge noise of the laser.

combination of the intra- and intermode V–V energy transfer rates and, thus, the rate must be much less dependent on the laser fluence than the observed one.

It has been suggested by Sheorey and Flynn[2] that a rapid accumulation of population in the $\nu_1 + \nu_3$ or $\nu_4 + \nu_3$ level through the resonant process:

$$CH_3F(\nu_1) + CH_3F(\nu_3) \longrightarrow CH_3F(\nu_1 + \nu_3) + CH_3F(0) \qquad (3)$$

results in an initial rapid rise of the emission due to the transition $\nu_1 + \nu_3 \rightarrow \nu_3$. However, the population in the ν_1 or ν_4 level is limited to the amount in equilibrium at room temperature, so that it would be difficult to explain the significant increase of the fluorescence intensity just after the excitation with a high laser fluence. Moreover, even if Eqn (3) contributes to the initial rapid rise of the 3-μm emission, the emission intensity must exceed the initial value in the later stage since populations in the ν_1 and ν_4 levels should grow due to the mechanism of

Eqn (1). This expectation was not realized in the present experiment using strong laser excitation.

The observed phenomenon on the ν_3 emission of CH_3F excited by the TEA CO_2 laser may not be attributed to a multiple photon absorption. The 3-μm emission of CH_3F was induced by irradiation with only two CO_2 laser lines, i.e. the 9.4-μm P(20) and the 10.2-μm R(20) lines. Of these lines, the latter induced the emission with its intensity being 1/100 that of the former. It is well known that the frequency of the 9.4-μm P(20) line is near-resonant to the ${}^qQ_K(12)(K=1, 2)$ $v=0\rightarrow 1$ transition of the ν_3 mode[13]. Thus, the linear resonant absorption in the ν_3 mode must be the major factor which determines the initial condition of the laser excitation.

Dispersed fluorescence spectra of ν_3 overtone and C—H stretching bands

Figure 3 shows the time-resolved fluorescence spectra of the ν_3 overtone band taken at intervals of 0.01 μm. Since the wavelength resolution of the monochromator is not sufficient to separate each vibration–rotation line, the observed spectra of the $\nu_3=2\rightarrow 0$, $3\rightarrow 2$ and $4\rightarrow 2$ transitions of the ν_3 overtone overlap with each other. The intensity of the spectral line for the vibration–rotation transition $v'J'K'\rightarrow v''J''K''$ of a symmetric top molecule is described as

$$I_{v'J'K'}^{v''J''K''} = C^{\mathrm{em}}(\omega_{v'J'K'}^{v''J''K''})^4 S_{J'K'}^{J''K''}(g_{J'K'}/2J'+1)g_{J'K'}^{s} \times \frac{\exp[-hcF(J'K')/kT_{\mathrm{R}}]}{Q_{\mathrm{R}}} |M_{v'}^{v''}|^2 N_{v'} \tag{4}$$

where the notations are defined as follows:

C^{em}, a constant ($=64\,\omega^4 c/3$);
$\omega_{v'J'K'}^{v''J''K''}$, wavenumber of the $v'J'K'\rightarrow v''J''K''$ transition $[=F(J'K')-F(J''K'')+G(v')-G(v'')]$;
$S_{J'K'}^{J''K''}$, angular part of the dipole moment matrix element;
$M_{v'}^{v''}$, vibrational contribution to the dipole matrix element;
T_{R} and Q_{R}, rotational temperature and rotational partition function, respectively;
$g_{J'K'}$ and $g_{J'K'}^{s}$, degeneracy of the $J'K'$ state and spin degeneracy, respectively;
$N_{v'}$, population density in v' level of the relevant vibrational mode.

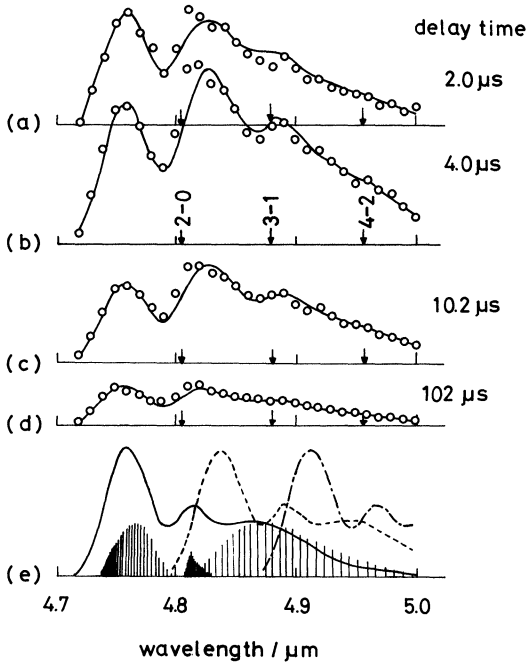

Figure 3 Dispersed time-resolved fluorescence spectra of the ν_3 overtone band of CH_3F at 0.5 Torr excited by 9.4-μm P(20) CO_2 laser line with the fluence of 0.52 J cm^{-2}. The spectra taken at the delay times of 2.0, 4.0, 10.2 and 102 μs are shown in frames (a)–(d), respectively. The calculated contributions of respective vibrational transitions of $\nu_3 = 2 \rightarrow 0$, $3 \rightarrow 1$ and $4 \rightarrow 2$ are given in (e) in which each rotational line is shown in only for $2 \rightarrow 0$ band.

Equation (43) can be reformed by introducing a function $U(\nu'J'K')$ as:

$$I_{\nu'J'K'}^{\nu''J''K''} = u(\nu'J'K')(|M_{\nu''}^{\nu''}|^2 N_{\nu'}) \tag{5}$$

If the monochromator which is set at a wavenumber ω_i has a spectral slit function $f(\omega_i, \omega)$, the observed emission intensity at this wavenumber is described as:

$$I(\omega_i) = \sum_{\nu'} \sum_{J'K'} u(\nu'J'K') f(\omega_i, \omega_{\nu'J'K'}^{\nu''J''K''})(|M_{\nu''}^{\nu''}|^2 N_{\nu'})$$

$$= \sum_{\nu''} U(\nu', \omega_i)(|M_{\nu''}^{\nu''}|^2 N_{\nu'}). \tag{6}$$

Thus, by defining $u(v'J'K')$ for vibrational transition from the v' level, the population multiplied by the dipole transition matrix element can be determined from the observed emission spectrum. The function $U(v', \omega_i)$ in the present experimental condition is given in Figure 3(e) in which bars indicate the relative magnitude of $\Sigma_{K'}u(v'J'K')$ for $v' = 2 \rightarrow 0$ transition of the ν_3 mode. In Figure 3 the calculated spectrum is also given assuming relative values for $|M_{v''}^{v'}|^2 N_{v'}$ from which the spectrum best fitted to the observed one is obtained. The relative fluorescence intensity from each of the $2\nu_3$, $3\nu_3$ and $4\nu_3$ levels is determined to be 1:0.4:0.02, 1:0.80:0.10, 1:0.80:0.10, and 1:0.50:0.02 for respective delay times of 2.0, 4.0, 10.2 and 102 μs after irradiation with the laser pulse. It is seen from Figure 3 that the populations in higher levels increase in the later stage indicating the 'up-the-ladder' intramode V–V energy transfer pumping. Since the spectrum calculated by Eqn (6) agrees very well with the observed ν_3 overtone emission spectrum, in the later experiments, the emissions at three wavelengths are selected for determination of the relative populations in the $2\nu_3$, $3\nu_3$ and $4\nu_3$ levels, i.e. the relative fluorescence intensities I_2, I_3 and I_4 from respective vibrational levels of $\nu_3 = 2$, 3 and 4 in the ν_3 mode are determined as follows:

$$I_2 = I_{4.76}/U(2, 4.76), \tag{7a}$$

$$I_3 = [I_{4.84} - U(2, 4.84)I_2]/U(3, 4.84), \tag{7b}$$

$$I_4 = [I_{4.92} - U(2, 4.92)I_2 - U(3, 4.92)I_3]/U(4, 4.92), \tag{7c}$$

where the observed fluorescence intensities at 4.76, 4.84 and 4.92 μm are denoted as $I_{4.76}$, $I_{4.84}$ and $I_{4.92}$, respectively.

The time-resolved fluorescence spectrum of the C—H stretching bands taken at the interval of 0.01 μm in the region from 3.19 to 3.59 μm is shown in Figure 4. The spectral analysis of the band is very complicated, since the emission is composed of a number of vibrational transitions, which densely overlap with each other. In Figure 4(d), the calculated spectrum for each vibrational transition is given on the basis of the data reported by Gigure and Overend[14]. Recently, Graner and coworkers[5,6] have reported a new set for the assignment: ν_1, $2\nu_2$, $2\nu_5^0$ for A_1 symmetry and ν_4, $\nu_2 + \nu_5$, $2\nu_5^2$ for E symmetry. According to their analysis, these vibrational states form a group of Fermi-coupled states in each symmetry and moreover, there are many Coriolis-coupled rotational levels belonging to different vibrational

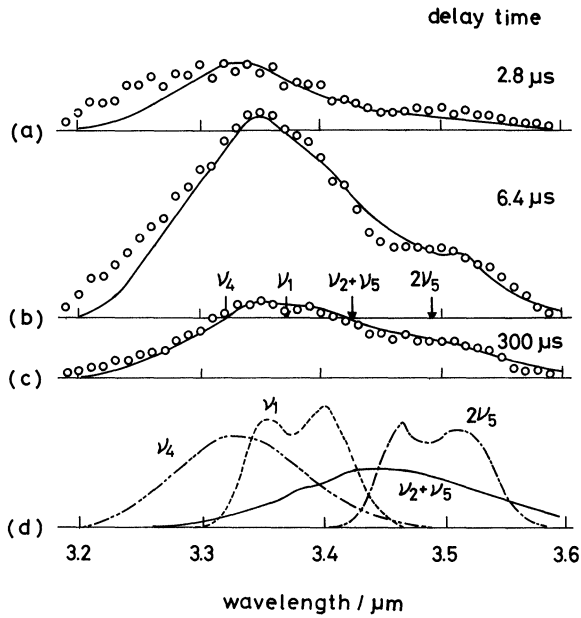

Figure 4 Dispersed fluorescence spectra of CH_3F in the 3-μm region under the same conditions as those given in Figure 3. Frames (a)–(c) are the spectra taken at the delay times of 2.8, 6.4 and 300 μs, respectively. In (d), the contributions of respective vibrational transitions are given.

states. Therefore, it is difficult to estimate the extent of the contribution of respective vibrational states to the observed fluorescence spectrum. Nevertheless, in a shorter wavelength region, the ν_4 vibration band is isolated from other bands due to relatively weak Fermi coupling with ν_1 vibration. Thus, it can be stated that the population rate in the ν_4 level in the early stage of the relaxation is larger than that in the ν_1, $2\nu_5$, . . . levels. In Figure 4 the observed spectral intensities in the wavelength range 3.2–3.3 μm are also found to be larger than those of the calculation. This might be attributable to a perturbation due to Coriolis coupling between the $3\nu_3$ and ν_4 state which has been pointed out already by Graner and Guelachvili[5].

The time-evolved emissions of the ν_3 overtone and those in the 3-μm region observed through the monochromator are shown in Figure 5. The emission data at the three wavelengths in Figure 5(a), (b) and (c) may yield the relative values for the populations in the $2\nu_3$, $3\nu_3$ and $4\nu_3$

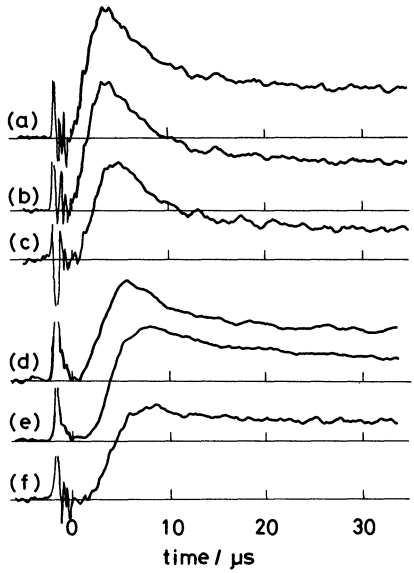

Figure 5 Time-evolved fluorescence intensities of CH_3F at 0.5 Torr after irradiation with the laser pulse of the fluence of 0.7 J cm^{-2}. An initial spike signal at $t = 0$ is due to the discharge noise of the laser. The wavelengths of the emissions are 4.76(a), 4.84(b), 4.92(c), 3.29(d), 3.43(e) and 3.52 μm (f), respectively.

states, respectively, on the basis of Eqns (7a)–(7c). The $2\nu_3$ population increases quickly to a peak which decays with an initial large rate. The population in the $3\nu_3$ level behaves in a way similar to that in the $2\nu_3$ level. The time-evolved emissions at 3.29, 3.43 and 3.52 μm are also shown in Figure 5(d)–(f). Referring to the spectrum given in Figure 4, the emission at the shortest wavelength can be interpreted as the contribution of population in the ν_4 level, while the data at the other two wavelengths are due to the densely overlapped emission bands from the ν_1, $2\nu_5$, $\nu_2 + \nu_5$ and $2\nu_2$ level. The emission at 3.29 μm rises quickly to form a peak in the early stages of relaxation. This behavior is common to that observed in the ν_3 overtone. Emission in the longer wavelength region rises slightly after increase of the emission intensity at a shorter wavelength, reaching an almost constant intensity, although it does not form a clear peak. This finding implies that the kinetics for the ν_4 population are different from those of the other levels; ν_1, $2\nu_5$, $\nu_2 + \nu_5$ and $2\nu_2$. These data will be discussed by comparison with the computer modelling of the relaxation kinetics.

Average number of photons absorbed per CH_3F molecule

The average number of laser photons absorbed per CH_3F molecule, $\langle n \rangle$, has been determined from observation of the intensity attenuation of the laser beam which passes through the CH_3F gas in a cell 1 m in length. Figure 6 indicates that $\langle n \rangle$ is dependent on the laser fluence as well as on the pressure. The value of $\langle n \rangle$ is defined by:

$$\langle n \rangle = \int [\sigma i(t)/nhc\omega]) N_0^L - N_1^L) dt, \tag{8}$$

where N is the number density of CH_3F, and N_0^L and N_1^L are those in the ground and excited levels, respectively, which may interact with the laser field, $I(t)$ is the laser intensity at time t, σ is the absorption cross section, and ω is the laser frequency. Using the reported values of the absorption cross-section[13] and the rotational relaxation rate constant[15] assuming that the ${}^qQ_1(12)$ and ${}^qQ_2(12)$ transitions to be resonant with the CO_2 laser line, it was impossible to reproduce the data given in Figure 6 based on Eqn (8) combined with the kinetic scheme described later. This is probably due to the power broadening of spectral lines and the collision-assisted multiple photon absorption. A value of $\langle n \rangle$ exceeding 0.5 at higher fluences is attributable to the fact that CH_3F excited to the ν_3 level makes collisional–rotational transitions to levels

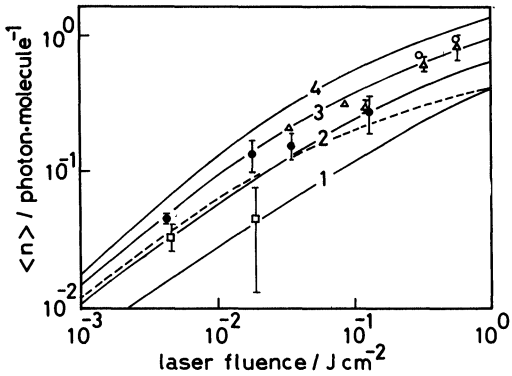

Figure 6 Observed and calculated average number of laser photons absorbed per CH_3F molecule as a function of the laser fluence. (1) 0.1(□); (2) 0.25 (●); (3) 0.5 (△); (4) 1.0 Torr (○). Broken line represents the calculated result for 0.5 Torr assuming $f = f_0$. Solid lines (1), (2), (3) and (4) are the calculated values for CH_3F at 0.1, 0.25, 0.5 and 1.0 Torr, respectively.

which enable CH_3F to absorb another photon to attain the $2\nu_3$ level during the laser pulse. This has been demonstrated in the CO_2 laser irradiation of the CH_3F/Ar mixture[16].

Table I Frequency difference in MHz of the rotation–vibration transitions of the ν_3 mode from the laser line, 9.4 μm $P(20)$[a].

	$\nu_3 = 0 \rightarrow 1$				$\nu_3 = 1 \rightarrow 2$	$\nu_3 = 2 \rightarrow 3$	$\nu_3 = 3 \rightarrow 4$
K	$^qP_K(1)$	$^qQ_K(11)$	$^qQ_K(12)$	$^qQ_K(13)$	$^qR_K(8)$	$^qR_K(20)$	$^qR_K(35)$
0	1587				1726	3632	−7047
1		8070	−28.8	−8786	1745	3641	−7070
2		8152	43.8	−8724	1830	3669	−7100
3		8295	171	−8615	1972	3715	−7166
4		8508	360	−8450	2170	3779	−7259
5		8801	625	−8217	2426	3861	−7378
6		9192	980	−7900	2738	3962	−7524
7		9700	1445	−7480	3107	4081	−7696
8			2043	−6935	3533	4218	−7894
9			2799	−6238		4373	−8119

[a] The laser frequency ν_L is 31 383 905.6 MHz determined by Chang[13], and the rotation–vibration transition frequencies are obtained based on the molecular constants given by Freund *et al.*[18]

The pressure dependence of $\langle n \rangle$ is attributable to the collision broadening of the absorption spectral line and also to the collision-induced rotational transitions which suppress saturation of the stimulated transitions. As shown in Table I, the laser line of 9.4 μm P(20) is near resonant to a number of transitions of $\nu_3 = 0 \rightarrow 1$, $1 \rightarrow 2$, $2 \rightarrow 3$ etc., in which ν_3 denotes the vibrational quantum number of the ν_3 mode. The absorption cross-section of the ith vibration–rotation transition in those listed in Table I is defined as follows, taking the collision broadening and the power broadening as well as the Doppler effect into account:

$$\sigma_i(\nu, I) = \int_{-\infty}^{+\infty} \frac{S_i \gamma_p}{\pi} \frac{1}{(\nu_i - \nu')^2 + \gamma_p^2 + \chi^2} f^D(\nu', \nu_i) d\nu', \tag{9}$$

where ν_i is the frequency of the ith line, γ_p, the collision frequency, χ, the Rabi frequency, $f_D(\nu', \nu_i)$, the Doppler line profile, and

$$S_i = (8\pi^3 \nu_i / 3hc)|M_i|^2. \tag{10}$$

in which $|M_i|$ is the transition diple moment. This value is described by the vibrational and rotational contributions:

$$|M_i|^2 = |M|^2 S_i. \tag{11}$$

The value of $|M|^2$ for the $\nu_3 = 0 \rightarrow 1$ transition of CH_3F was determined by Saeki *et al.* to be 0.1953D[17].

Owing to multimode oscillation of the present TEA CO_2 laser, the laser pulse is composed of a number of lines whose frequency distributes over a range as wide as 1 GHz. Assuming the Lorentz function to describe the frequency distribution of the CO_2 laser line, the effective absorption cross section due to the ith transition of CH_3F for the laser line is defined as:

$$\sigma_i(\bar{\nu}_L) = \int \sigma_i(\nu) g(\nu) \mathrm{d}\nu \Big/ \int g(\nu) \mathrm{d}\nu \tag{12}$$

where $\bar{\nu}_L$ is the mean frequency of the laser line. The average number of photons absorbed per CH_3F molecule may be calculated by the equation:

$$\langle n \rangle = \sum_i \int [\sigma_i(\bar{\nu}_L) I(t) / N h \bar{\nu}_L] (N^i_{\text{lower}} - N^i_{\text{upper}}) \mathrm{d}t \tag{13}$$

where N^i_{lower} and N^i_{lower} are the number densities of CH_3F molecules in the lower and upper levels of the ith transition, respectively, and N is the total number density of CH_3F. The summation in Eqn (13) must be made on respective transitions of the ν_3 vibration listed in Table I, and N^i values are the solution of the coupled rate equations that describe the stimulated transitions and the rotational and vibrational energy transfer collisions. If these rate equations are formulated for each population in respective levels of J, K states relating to the stimulated transition induced by laser irradiation, the number of coupled rate equations to be solved is very large, and it becomes physically unrealistic. Thus, we define a parameter which represents an average absorption cross-section for the $\nu_3 = \nu'' \rightarrow \nu'$ transition as follows:

$$\sigma_{\nu''} = \sum_i \sigma_i(\bar{\nu}_L) f_i \Big/ \sum_i f_i, \tag{14}$$

where f_i is the fraction of population in the lower rotational level of the vibrational state ν'' for the ith transition. Assuming the average effective

(apparent) cross-section defined above, the kinetic equation is formulated to describe the laser-induced stimulated transitions and the collisional rotation as well as vibration transfer processes. It is assumed that a fraction of the population in the v'' states possesses the absorption cross section of Eqn (12) and this fraction is a function of the laser fluence:

$$\begin{aligned} f &= f_0 + aI(t), \quad \text{for } v_3 = 0 \\ f &= aI(t) \qquad\quad \text{for } v_3 = 1 \text{ and } 2 \end{aligned} \tag{15}$$

where f_0 is estimated to be 0.042 assuming the thermal rotational equilibrium distribution at room temperature, and $I(t)$ is the laser power at time t, and a coefficient a is selected so that the calculated value of $\langle n \rangle$ fits with the observed values given in Figure 6. If the fraction f introduced in Eqn (14) is a certain constant value independent of the laser power, the calculated result of $\langle n \rangle$ may not reproduce the experimental data which is a function of the laser fluence as well as the CH_3F pressure. Thus, the laser stimulation scheme presented above is adopted to model the excitation and relation kinetics of laser-irradiated CH_3F molecules.

Excitation and relaxation kinetics

Simultaneous differential equations are formulated to describe the excitation and relaxation kinetics of CH_3F whose ν_3 mode is excited by irradiation with the 9.4-μm P(20) line of the TEA CO_2 laser pulse. The vibrational levels taken into consideration are summarized in Table II. For convenience, one vibrational level which represents both the ν_2 and ν_5 levels is assumed by introducing the increased degeneracy and is designated ν_{25}—the energy level is the average of ν_2 and ν_5 weighted by their degeneracies. A similar treatment was taken for levels in the C—H stretching region. Referring to the emission spectrum given in Figure 4, it is seen that one cannot discriminate respective contributions of the ν_1, $2\nu_2$, $\nu_2 + \nu_5$, and $2\nu_5$ levels to the observed emission spectrum. Moreover, according to the high resolution spectroscopic studies, these vibrational states couple strongly with each other by Coriolis and Fermi interactions[5,6]. Therefore, five vibrational states are presented by one state ν_{125} whose degeneracy is seven in the present model. The vibrational frequencies listed in Table II are taken

from Freund *et al.*[18] for ν_3, Gigure and Overend[14] for ν_1 and ν_4 and Shimanouchi[19] for the others.

Table II Vibrational energy levels of CH_3F taken into account in the kinetic model calculation.

Level number	Level	Energy (cm^{-1})	Degeneracy
1	ν_3	1049	1
2	ν_6	1182	2
3	ν_{25}[a]	1466	3
4	$2\nu_3$	2081	1
5	$\nu_3 + \nu_6$	2230	2
6	$2\nu_6$	2348	3
7	$\nu_3 + \nu_{25}$	2515	3
8	$\nu_6 + \nu_{25}$	2634	6
9	ν_{125}[b]	2914	7
10	ν_4	3009	2
11	$3\nu_3$	3098	1
12	$\nu_3 + \nu_{125}$	3963	7
13	$\nu_3 + \nu_4$	4058	2
14	$4\nu_3$	4099	1
0	0	0	1

[a] $\nu_2(A_1)$ 1464, $\nu_5(E)$ 1467 cm^{-1}.
[b] $\nu_1(A_1)$ 2966, $2\nu_2(A_1)$ 2926, $2\nu_5(A_1)$ 2863, $\nu_2 + \nu_5(E)$ 2927, $2\nu_5(E)$ 2922 cm^{-1}.

In Table III, the energy transfer processes taken into consideration are summarized together with the non-resonant energy ΔE, and the rate constant assigned to each process. The energy transfer process may be categorized into three groups: intermolecular intramode V–V energy transfer, intra- or intermolecular intermode V–V, and V–T/R energy transfer. Of intramode V–V energy transfers, the energy transfer from ν_{25} to $2\nu_5$ is the assumed to occur through the intermediate state of $\nu_2 + \nu_5$, since the $2\nu_5$ level is Fermi coupled and greatly shifted. The intermode V–V energy transfers considered here are all involved in the relaxation mechanism proposed by Sheorey and Flynn[2] and also by Apkarian and Weitz[3], except for process [18] (in Table III) which is the direct energy transfer between $3\nu_3$ and ν_4. This latter process is assumed to occur collisionally and will be discussed later. V–T/R energy transfer is assumed to occur from ν_3 and ν_6 modes. Most of the rate constants for the energy transfer processes [1]–[23] are taken from the papers of Sheorey and Flynn[2] and Apkarian and Weitz[3]. However, there remain many unknown rate constants that must have been

Table III Energy transfer processes assumed in the kinetic model calculation[a].

Process	$\Delta E(cm^{-1})$	Rate constant (s^{-1} $Torr^{-1}$)
Intramode V–V energy transfer		
[1] $(\nu_3) + (\nu_3) \rightarrow (2\nu_3) + (0)$	+17	$k_{u3} = 2.4 \times 10^{6}$ [b]
[2] $(2\nu_3) + (\nu_3) \rightarrow (3\nu_3) + (0)$	+32	$k_{u33} = 3.7 \times 10^{6}$ [d]
[3] $(3\nu_3) + (\nu_3) \rightarrow (4\nu_3) + (0)$	+48	$k_{u333} = 4.9 \times 10^{6}$ [d]
[4] $(\nu_6) + (\nu_6) \rightarrow (2\nu_6) + (0)$	+16	$k_{u6} = 1 \times 10^{6}$ [f]
[5] $(\nu_{25}) + (\nu_{25}) \rightarrow (\nu_{125}) + (0)$	0	$k_{u25} = 1.6 \times 10^{6}$ [c]
[6] $(\nu_3) + (\nu_6) \rightarrow (\nu_3 + \nu_6) + (0)$	+1	$k_{u36} = 1 \times 10^{6}$ [f]
[7] $(\nu_3) + (\nu_{25}) \rightarrow (\nu_3 + \nu_{25}) + (0)$	0	$k_{u23} = 1 \times 10^{6}$ [f]
[8] $(\nu_3) + (\nu_{125}) \rightarrow (\nu_3 + \nu_{125}) + (0)$	0	$k_{u13} = 1 \times 10^{6}$ [f]
[9] $(\nu_6) + (\nu_{25}) \rightarrow (\nu_6 + \nu_{25}) + (0)$	+14	$k_{u26} = 1 \times 10^{6}$ [f]
[10] $(\nu_3) + (\nu_4) \rightarrow (\nu_3 + \nu_4) + (0)$	0	$k_{u34} = 1 \times 10^{6}$ [f]
Intermode V–V energy transfer		
[11] $(\nu_3) + M \rightarrow (\nu_6) + M$	−133	$k_{3,6} = 2.9 \times 10^{5}$ [b]
[12] $(\nu_6) + M \rightarrow (\nu_{25}) + M$	−284	$k_{6,2} = 7.0 \times 10^{4}$ [b]
[13] $(2\nu_3) + M \rightarrow (\nu_3 + \nu_6) + M$	−149	$k_{33,36} = 5.8 \times 10^{5}$ [d]
[14] $(\nu_3 + \nu_6) + M \rightarrow (2\nu_6) + M$	−118	$k_{36,66} = 5.8 \times 10^{5}$ [d]
[15] $(2\nu_6) + M \rightarrow (\nu_6 + \nu_{25}) + M$	−286	$k_{66,26} = 1.4 \times 10^{5}$ [d]
[16] $(\nu_6 + \nu_{25}) + M \rightarrow (\nu_{125}) + M$	−280	$k_{26,1} = 1.4 \times 10^{5}$ [d]
[17] $(\nu_3 + \nu_6) + M \rightarrow (\nu_3 + \nu_{25}) + M$	−285	$k_{36,23} = 7.0 \times 10^{4}$ [e]
[18] $(\nu_3 + \nu_{25}) + M \rightarrow (\nu_6 + \nu_{25}) + M$	−119	$k_{23,26} = 2.9 \times 10^{5}$ [e]
[19] $(3\nu_3) + M \rightarrow (\nu_4) + M$	+89	$k_{333,4} = 5 \times 10^{5}$ [f]
[20] $(\nu_{125}) + M \rightarrow (\nu_4) + M$	+95	$k_{1,4} = 1 \times 10^{6}$ [f]
V–T/R energy transfer		
[21] $(n\nu_3) + M \rightarrow (n - 1\ \nu_3) + M$	+1049	$k_{t3} = 3.7 \times 10^{2} n$ [g]
[22] $(n\nu_6) + M \rightarrow (n - 1\ \nu_6) + M$	+1182	$k_{t6} = 8.7 \times 10^{2} n$ [g]

[a] CH_3F in ν_i level is denoted as (ν_i), while CH_3F in the ground state as (0) and CH_3F as a third body collider as M.

[b] Determined by Sheorey and Flynn[2].

[c] Determined by Apkarian and Weitz[3].

[d] Estimated from the data of Sheorey and Flynn[2] based on the Landau–Teller rule.

[e] Estimated from the data of Sheorey and Flynn[2].

[f] Assumed value.

[g] Determined by Weitz and Flynn[23]; here the ratio of k_{t3} ro k_{t6} is assumed as the one calculated by the SSH theory.

[h] Assuming the detailed balancing rule, the rate constant for the backward reaction is defined as k_{di} for k_{ui}, $k_{j,i}$ for $k_{i,j}$, and k_{tbi} for k_{ti}.

estimated on a reasonable basis. Regarding the intramode V–V energy transfers, the rate constants for $2\nu_3 \rightarrow 3\nu_3$ and $3\nu_3 \rightarrow 4\nu_3$ are estimated from that for $\nu_3 \rightarrow 2\nu_3$ determined by Sheorey and Flynn[2] assuming the Landau–Teller rule, where the effect of the non-resonance on the rate constant is disregarded, so that possibly the rate constants are slightly

overestimated. For the other intramode V–V energy transfer rates, the value of $1 \times 10^6\,s^{-1}\,Torr^{-1}$ is assumed for the first step of the "up-the-ladder" process, since the rates for these V–V energy transfers must be close to the one for $\nu_{25} \rightarrow \nu_2 + \nu_5$ which has been determined by Apkarian and Weitz[3] or to another intramode V–V energy transfer rate which is of the order of $10^6\,s^{-1}\,Torr^{-1}$. As for the intermode V–V energy transfers, based on the data of Sheorey and Flynn[2] for $\nu_3 \rightarrow \nu_6$ and $\nu_6 \rightarrow \nu_{25}$, the other V–V energy transfer rates through the combination levels such as $2\nu_3 \rightarrow \nu_3 + \nu_6$, $\nu_3 + \nu_6 \rightarrow 2\nu_6$ etc. are also estimated by the Landau–Teller rule. For the intermode V–V energy transfers of $3\nu_3 \leftrightarrow \nu_4$ and $\nu_4 \leftrightarrow \nu_{125}$, the values listed in Table III are adopted in the trial calculation. The effect of the direct energy transfer from $3\nu_3$ to ν_4 and other states on the entire relaxation is one of the major subjects of this paper, so that the adequacy of these rate constants will be discussed later.

Taking the energy transfer processes [1]–[21] into account, the kinetic equations are formulated to describe the time-dependent population in each vibrational level among 14 levels in the course of the relaxation which starts by laser excitation of the ν_3 mode at the time origin. In the equations, the number density in ith level is denoted as N_i in which the level number i is defined in Table I except in $i = 0$ which means the ground state. The total number density of CH_3F is defined as $N = \Sigma_i N_i$.

For the excitation process, it is assumed that a fraction of $N_i (i = 0, 4,$ or 11) may interact with the laser radiation field of 9.4-μm P(20) line, and that the average absorption cross section σ_j is common for the transition from the $j\nu_3$ state to the $(j+1)\nu_3$. If the parameter f_j is introduced as an equilibrium fraction of populations in these rotational levels of the relevant vibrational state, the rate equation for the population, N_i^{Lj}, in the rotational levels of the ith state which makes a stimulated transition to or from the kth state is formulated as follows:

$$\begin{aligned} dN_i^{Lj}/dt = & -(\sigma_j I/h\nu)(N_i^{Lj} - n_k^{Lj}) + \{-k_{rot} N_i^{Lj} N \\ & + [f_j/(1 - f_j)] k_{rot} (N_i - N_i^{Lj})\} + f_j R_i, \end{aligned} \tag{16}$$

where $j = 1$, 2 and 3 corresponds to the transitions of $i = 0 \rightarrow 1$, $1 \rightarrow 4$ and $4 \rightarrow 11$, respectively, and k_{rot} is the rate constant of transitions from rotational levels interacting with the laser photon field to the other rotational levels, and is assumed to be a common value of

$1.25 \times 10^8\,s^{-1}\,Torr^{-1}$ [19] for all rotational levels, and R_i is the overall rate of the collisional vibrational transition to the ith state from the other vibrational states, i.e.:

$$\begin{aligned} R_0 = {} & (-k_{d3}N_4N_0 + k_{u3}N_1N_1) + (-k_{d33}N_{11}N_0 + k_{u33}N_4N_1) \\ & + (-k_{d333}N_{14}N_0 + k_{u333}N_{11}N_1) + (-k_{d6}N_6N_0 + k_{u6}N_2N_2) \\ & + (-k_{d25}N_9N_0 + k_{u25}N_3N_3) + (-k_{d13}N_{14}N_0 + k_{u13}N_9N_1) \\ & + (-k_{d34}N_{13}N_0 + k_{u34}N_{10}N_1) + (-k_{d36}N_5N_0 + k_{u36}N_2N_1) \\ & + (-k_{d26}N_8N_0 + k_{u26}N_3N_2) + (-k_{d23}N_7N_0 + k_{u23}N_3N_1) \\ & + (-k_{tb3}N_0N + k_{t3}N_1N) + (-k_{tb6}N_0N + k_{t6}N_2N) \end{aligned} \tag{17}$$

$$\begin{aligned} R_1 = {} & 2(-k_{u3}N_1N_1 + k_{d3}N_4N_0) + (-k_{u33}N_1N_4 + k_{d33}N_1N_0) \\ & + (-k_{u333}N_{11}N_1 + k_{d333}N_{14}N_0) + (-k_{u13}N_9N_1 + k_{d13}N_{12}N_0) \\ & + (-k_{u34}N_{10}N_1 + k_{d34}N_{13}N_0) + (-k_{u36}N_2N_1 + k_{d36}N_5N_0) \\ & + (-k_{u23}N_3N_1 + k_{d23}N_7N_0) + (-k_{3,6}N_1N + k_{6,3}N_2N) \\ & + (-k_{t3}N_1N + k_{tb3}N_0N) + (2k_{t3}N_4N - 2k_{tb3}N_1N) \\ & + (-k_{t6}N_5N + k_{tb6}N_1N) \end{aligned} \tag{18}$$

$$\begin{aligned} R_4 = {} & (-k_{d3}N_4N_0 + k_{u3}N_1N_1) + (-k_{u33}N_4N1 + k_{d33}N_{11}N_0) \\ & + (-k_{33,36}N_4N + k_{36,33}N_5N) + (-2k_{t3}N_4N + 2k_{tb3}N_1N) \\ & + (3k_{t3}N_{11}N - 3k_{tb3}N_4N) \end{aligned} \tag{19}$$

$$R_{11} = (-k_{d34}N_{13}N_0 + k_{u34}N_{10}N_1) + (-3k_{t3}N_{11}N + 3k_{tb3}N_4N) \tag{20}$$

The kinetic equations for respective vibrational levels are formulated according to the mechanism described in Table III as follows:

$$dN_1/dt = (\sigma_1 I/h\nu)(N_0^{L1} - N_1^{L1}) - (\sigma_2 I/h\nu)(N_1^{L2} - N_2^{L2}) + R_1 \tag{21}$$

$$\begin{aligned} dN_2/dt = {} & 2(-k_{u6}N_2N_2 + k_{d6}N_6N_0) + (-k_{u36}N_1N_2 + k_{d36}N_5N_0) \\ & + (-k_{u26}N_2N_3 + k_{d26}N_8N_0) + (-k_{6,3}N_2N + k_{3,6}N_1N) \\ & + (-k_{6,2}N_2N + k_{2,6}N_3N) + (-k_{t6}N_2N + k_{tb6}N_0N) \\ & + (k_{t3}N_5N - k_{tb3}N_2N) + (2k_{t6}N_6N - 2k_{tb6}N_2N) \end{aligned} \tag{22}$$

$$\begin{aligned} dN_3/dt = {} & 2(-k_{u2}N_3N_3 + k_{d2}N_9N_0) + (-k_{u23}N_1N_3 + k_{d23}N_7N_0) \\ & + (-k_{u26}N_2N_3 + k_{62}N_8N) + (-k_{2,6}N_3N + k_{6,2}N_2N) \\ & + (k_{t3}N_7N - k_{tb3}N_3N) + (k_{t6}N_8N - k_{tb6}N_3N) \end{aligned} \tag{23}$$

$$dN_4/dt = (\sigma_2 I/h\nu)(N_1^{L2} - N_4^{L2}) - (\sigma_3 I/h\nu)(N_4^{L3} - N_{11}^{L3}) + R_4 \tag{24}$$

$$\begin{aligned} dN_5/dt = {} & (-k_{d36}N_5N_0 + k_{u36}N_2N_1) + (-k_{36,33}N_5N + k_{33,36}N_4N) \\ & + (-k_{36,23}N_5N + k_{23,36}N_7N) + (-k_{36,66}N_5N + k_{66,36}N_6N) \\ & + (-k_{t3}N_5N + k_{tb3}N_2N) + (-k_{t6}N_5N + k_{tb6}N_1N) \end{aligned} \tag{25}$$

$$\begin{aligned} dN_6/dt = {} & (-k_{d6}N_6N_0 + k_{u6}N_2N_2) + (-k_{66,36}N_6N + k_{36,66}N_5N) \\ & + (-k_{66,26}N_6N + k_{26,66}N_8N) + (-2k_{t6}N_6N + 2k_{tb6}N_2N) \end{aligned} \tag{26}$$

$$dN_7/dt = (-k_{d23}N_7N_0 + k_{u23}N_3N_1) + (-k_{23,36}N_7N + k_{36,23}N_5N) + (-k_{23,26}N_7N + k_{26,23}N_8N) + (-k_{t3}N_7N + k_{tb3}N_3N) \quad (27)$$

$$dN_8/dt = (-k_{d26}N_8N_0 + k_{u26}N_2N_3) + (-k_{26,1}N_8N + k_{1,26}N_9N) + (-k_{26,23}N_8N + k_{23,26}N_7N) + (-k_{26,66}N_8N + k_{66,26}N_6N) + (-k_{t6}N_8N + k_{tb6}N_3N) \quad (28)$$

$$dN_9/dt = (k_{u25}N_3N_3 - k_{d25}N_9N) + (-k_{u13}N_9N_1 + k_{d13}N_{12}N) + (k_{26,1}N_8N - k_{1,26}N_9N) + (-k_{1,4}N_9N + k_{4,1}N_{10}N) + (k_{t3}N_{12}N - k_{tb3}N_9N) \quad (29)$$

$$dN_{10}/dt = (-k_{u34}N_{10}N_1 + k_{d34}N_{13}N_0) + (-k_{4,333}N_{10}N + k_{333,4}N_{11}N) + (-k_{4,1}N_{10}N + k_{1,4}N_9N) + (k_{t3}N_{13}N - k_{tb3}N_9N) \quad (30)$$

$$dN_{11}/dt = (\sigma_3 I/h\nu)(N_4^{L3} - N_{11}^{L3}) + R_{11} \quad (31)$$

$$dN_{12}/dt = (-k_{d13}N_{12}N_0 + k_{u13}N_9N_1) + (-k_{t3}N_{12}N + k_{tb3}N_9N) \quad (32)$$

$$dN_{13}/dt = (-k_{d34}N_{13}N_0 + k_{u34}N_{10}N_1) + (-k_{t3}N_{13}N + k_{tb3}N_{10}N) \quad (33)$$

$$dN_{14}/dt = (-k_{d333}N_{14}N_0 + k_{u333}N_{11}N_1) + (-4k_{t3}N_{14}N + 4k_{tb3}N_{11}N) \quad (34)$$

The number density of the ground state may be derived by the relation

$$N_0 = N - \sum_{i=1}^{14} N_i. \quad (35)$$

These coupled differential Eqns (16), (21)–(34) were solved numerically by a Runge–Kutta–Gill method with the initial condition that the population distribution in respective vibrational levels at $t = 0$ is assumed to be in equilibrium at 295 K.

Comparison of kinetic calculation with LIF data

In Figure 7, the calculated fractional population changes in the $2\nu_3$ and $3\nu_3$ levels induced by laser irradiation are shown together with the observed overtone emission from each state. Here, the observed emission intensities from $2\nu_3$ at the laser fluence of $0.7\,J\,cm^{-2}$ are plotted so as to fit with the calculated ones in the later stage of relaxation. Thus, we may discuss the emission intensities from the $3\nu_3$ level relative to those from $2\nu_3$, and also the emission under a high

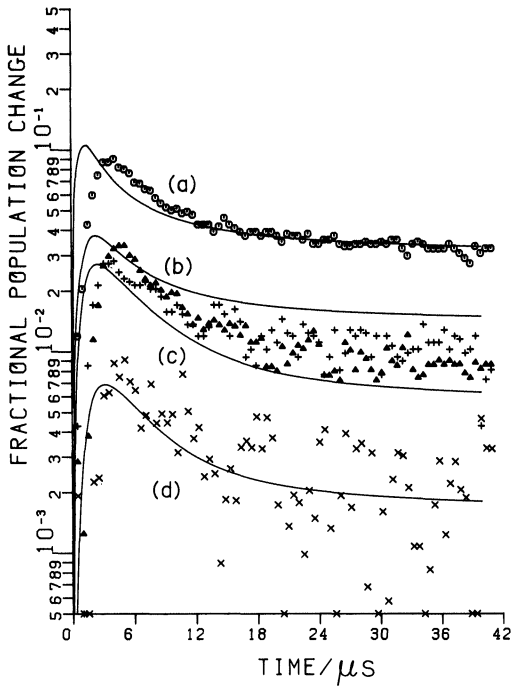

Figure 7 Observed and calculated fractional population changes in $2\nu_3$ and $3\nu_3$ levels of CH_3F at 0.5 Torr. The calculation was carried out based on the kinetic scheme described in Table III. The relative population is given by the $3\nu_3$ or $2\nu_3$ emission intensity. (a) and (b) $2\nu_3$ emission in excitation with fluence of 0.7 (○) and 0.097 J cm^{-2}(+), respectively; (c) and (d) $3\nu_3$ emission with 0.7 (△) and 0.097 J cm^{-2} (×), respectively. The observed $2\nu_3$ emission intensities are plotted in accord with the calculated values 10–40 μs after the laser pulse.

fluence irradiation relative to those under a low fluence. Due to the relatively slow response of the IR light detecting system, the emission intensities were found to increase with a rate smaller than that calculated. However, the observed relative intensities and the decay rates of the $2\nu_3$ emission are in good agreement with the calculated fractional population change in $2\nu_3$ level based on the model including the direct $3\nu_3 \longleftrightarrow \nu_4$ V–V energy transfer. The observed population change in $3\nu_3$, which is defined as an emission intensity from the $3\nu_3$ level relative to that from $2\nu_3$, is larger by a factor of 1.5 than the calculated population change. Nevertheless, it may be stated that the

present kinetic model calculation could reproduce the population kinetics determined by the LIF emission measurement.

Referring to the spectral analysis of the 3-μm emission band shown in Figure 4(d), the emission at the shortest wavelength 3.28 μm in this experiment is attributable to the ν_4 population, while the emission in the longer wavelength region, e.g. 3.52 μm is contributed from mainly $2\nu_2$, $\nu_2 + \nu_5$ and ν_5. Figure 8 shows the emission data together with the calculated results. Here, the observed ν_4 emission intensities at a later stage of the relaxation under the laser fluence of 0.7 J cm^{-2} are plotted to fit with the calculated ν_4 population. The ν_4 emission at 3.29 μm

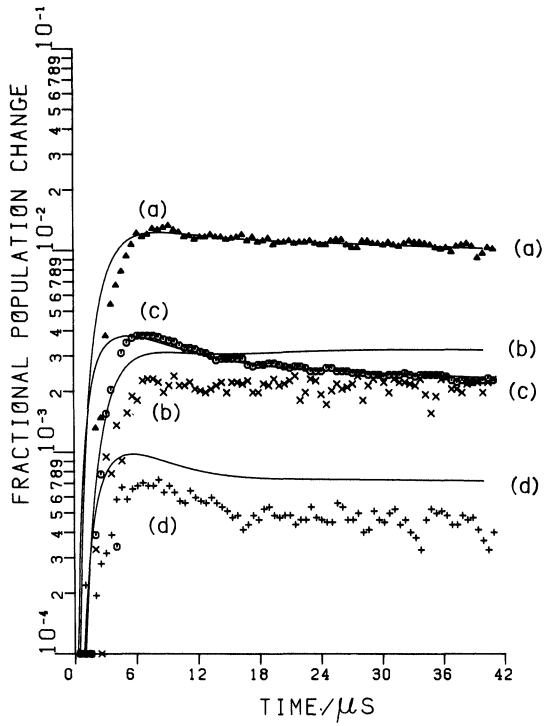

Figure 8 Observed and calculated fractional population changes in ν_4 and ν_{125} levels of CH_3F at 0.5 Torr. (a) and (b) ν_{125} emission at 3.52 μm in excitation with fluence of 0.7 (△) and 0.097 J cm^{-2} (×), respectively; (c) and (d) ν_4 emission at 3.29 μm in excitation with 0.7 (○) and 0.097 J cm^{-2} (+), respectively. The ν_{125} and ν_4 emission intensities at the fluence of 0.7 J cm^{-2} are plotted in accord with calculated values 10–40 μs after the laser pulse.

forms a peak at an initial stage which is reproduced in the calculation in spite of some disagreement in the increasing rate. This latter fact is probably due to insufficient response of the present IR light detecting system. The calculated ν_4 population in laser irradiation with a lower fluence, 0.097 J cm^{-2}, is almost in agreement with the observed emission intensity, although its relative magnitude is too small by a factor of 1.5. This implies that the kinetic model given in Table III may predict the dependence of the ν_4 emission on the irradiated laser fluence. The emission at 3.52 μm does not show a clear peak after the initial rapid rise, and it keeps almost a constant magnitude during several tens of microseconds. This observation is consistent with the present kinetic model, if it is admitted that the ν_1, $2\nu_5$ and $\nu_2 + \nu_5$ levels contribute to the 3.52-μm emission.

Of the rate constants assigned to energy transfer processes listed in Table III, the magnitudes of $k_{333,4}$ and $k_{1,4}$ are most ambiguous. The energy transfer between ν_1 and ν_4 must be very efficient, because some rotational levels of these vibrational states are coupled with each other due to Coriolis forces and furthermore large dipole matrices are expected because of the intense absorption of the ν_1 and ν_4 bands. Therefore, a large value, 1×10^6 s^{-1} Torr^{-1}, is assumed for a temporal value of $k_{1,4}$. The kinetic calculation was made assuming various values for $k_{333,4}$ in the range of 1×10^5–1×10^6 s^{-1} Torr^{-1}. Comparison of the calculated time-evolved populations with the observed emissions from $2\nu_3$, $3\nu_3$, ν_4 and $\nu_1/2\nu_2/\nu_2 + \nu_5/2\nu_5$ leads to the conclusion that $k_{333,4}$ must be between 5×10^5 and 1×10^6s^{-1} Torr^{-1}. Similarly, $k_{1,4}$ was changed by a factor of five assuming the fixed value for $k_{333,4}$ of 5×10^5 s^{-1} Torr^{-1}. However the calculated time-evolved populations in relevant vibrational states were found to be relatively insensitive to the magnitude of this rate constant. Thus, it was concluded that the set of rate constants given in Table III was satisfactory for quantitative discussion on the relaxation mechanism.

In Figure 9, the experimental decay data of emissions from the $2\nu_3$, $3\nu_3$ and ν_4 levels in the final stage of the relaxation are presented. The intensities of the $2\nu_3$ and ν_4 emission are normalized in a way similar to that shown in Figures 7 and 8, so that one may discuss the population changes in $3\nu_3$ relative to $2\nu_3$ and also those of ν_{125} to ν_4 using the calculated results given in Figure 9 as absolute values of the population changes in the respective states. Good agreement is seen between the observed emission decays and the kinetic model calculation in the later

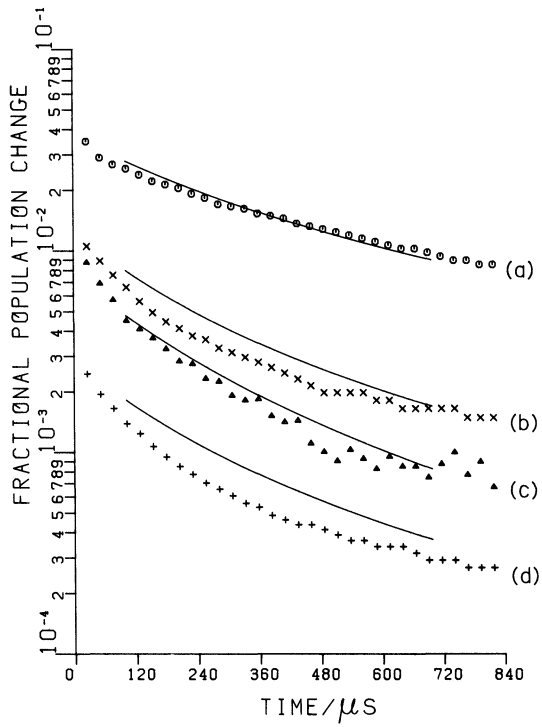

Figure 9 Observed and calculated fractional population changes in (a) $2\nu_3$ (○), (b) ν_{125} (×), (c) $3\nu_3$ (△), and (d) ν_4 (+) in the later stage of the relaxation of CH_3F excited with fluence of $0.7\,J\,cm^{-2}$ (see Figures 7 and 8).

stage of relaxation. Clearly, the observed decay of populations in the $2\nu_3$, $3\nu_3$ and ν_4 states is much faster than the V–T/R transfer, and is not simply exponential; the decay rate is reduced gradually in the later stage and the decay of the $2\nu_3$ emission is slower than those in the other higher states, ν_{125}, ν_4 and $3\nu_3$. These observations are reproduced well by the present kinetic model calculation.

Relaxation kinetic scheme with *versus* without $3\nu_3 \longleftrightarrow \nu_4$ V–V energy transfer

The kinetic rate Eqns (16), (21–34), which are formulated based on the energy transfer processes given in Table III, are solved numerically for two cases: under the initial conditions of weak and strong laser

excitation. Figures 10(a) and (b) show the calculated population changes in respective vibrational levels after the laser pulse excitation with the fluence of 0.001 J cm^2. The calculation was made on the basis of the kinetic mechanism with or without the $3\nu_3 \longleftrightarrow \nu_4$ V–V energy transfer. In the initial stage of relaxation, as shown in Figure 10(a), rapid increase of the populations in the ν_3, $2\nu_3$, $3\nu_3$ levels occurs indicating the laser excitation to these levels and the efficient intramode V–V energy transfers within the ν_3 mode. In the next stage, intermode V–V energy transfers from ν_3 to the other modes occur resulting in rapid reduction of populations in the ν_3 mode and increase of populations in the other states. In the case of the weak laser excitation, the $3\nu_3 \longleftrightarrow \nu_4$ V–V energy transfer may not affect the

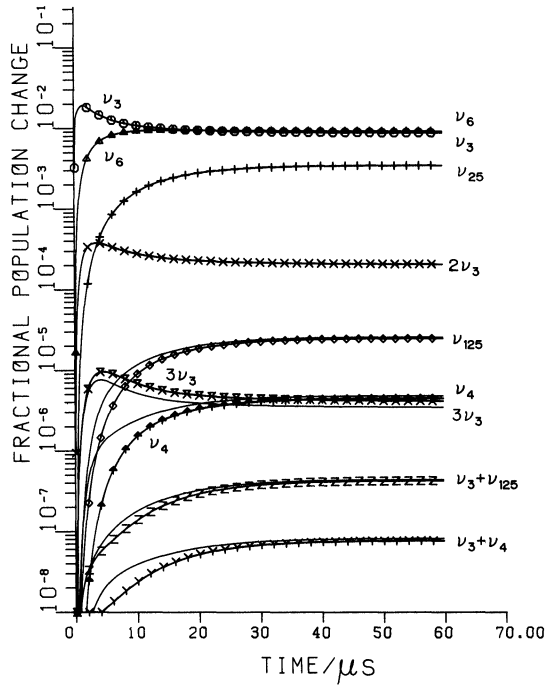

Figure 10 (a) Calculated fractional population changes in respective levels of CH_3F irradiated with the CO_2 laser pulse at the fluence of 0.001 J cm^{-2}. The curves marked with symbols show the results obtained based on the kinetic scheme without the $3\nu_3 \longleftrightarrow \nu_4$ V–V energy transfer, while those without symbols show the results with the above V–V energy transfer.

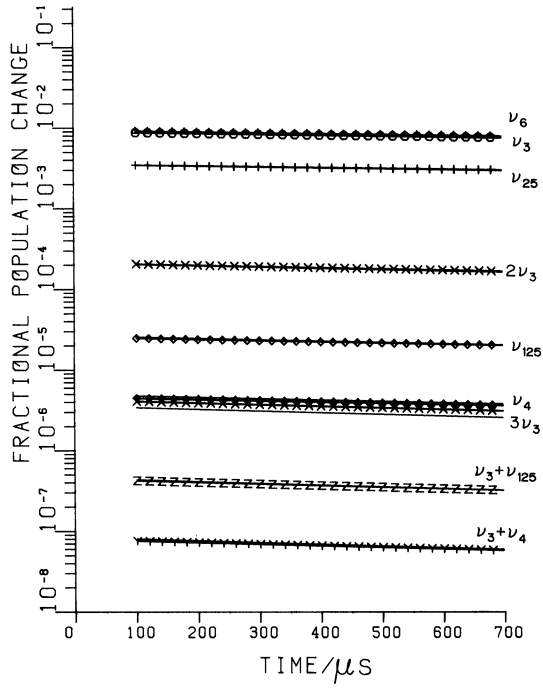

Figure 10 (b) Calculated fractional population changes of (a) in the later stage of the relaxation.

relaxation kinetics. In two mechanisms with and without the V–V energy transfer, the ν_4, ν_1, and other nearby states are populated with almost the same rate. Population in ν_4 is slightly accelerated by inclusion of the $3\nu_3 \longleftrightarrow \nu_4$ V–V energy transfer, but the major part of the population is caused by the energy flow mechanism in Eqn (1). In the later stage of the relaxation, the calculations based on either mechanism result in the same population kinetics at the respective levels. The population in each level is reduced exponentially with the common rate, which is defined from the V–T/R energy transfer rates of ν_3 and ν_6 modes. Thus, in weak laser excitation of ν_3 mode, the vibrational energy flow from ν_3 to ν_4 and ν_1 and other nearby levels occurs mainly through Eqn (1) and the contribution of Eqn (2) is relatively small.

In the case of strong laser excitation, a large energy is poured into the ν_3 mode, and the vibrational energy flow scheme from ν_3 to ν_4, ν_1,

and other levels is dependent significantly upon whether the kinetic model includes the $3\nu_3 \longleftrightarrow \nu_4$ energy transfer or not. Without the V–V energy transfer, the population kinetics are essentially the same as those given in Figure 10(a). The vibrational energy flows from ν_3 to ν_2, ν_5 through ν_6 and finally to ν_1 and ν_4 keeping the quasiequilibrium population distribution within each vibrational mode. In the later stage of the relaxation, as shown in Figure 10(d), populations in respective levels decrease exponentially against time with the V–T/R energy transfer rate. Contrary to this, if the $3\nu_3 \longleftrightarrow \nu_4$ V–V energy transfer is included in the kinetic mechanism, the population kinetics for respective levels differ significantly from those predicted based on the mechanism without the $3\nu_3 \longleftrightarrow \nu_4$ V–V energy transfer. The

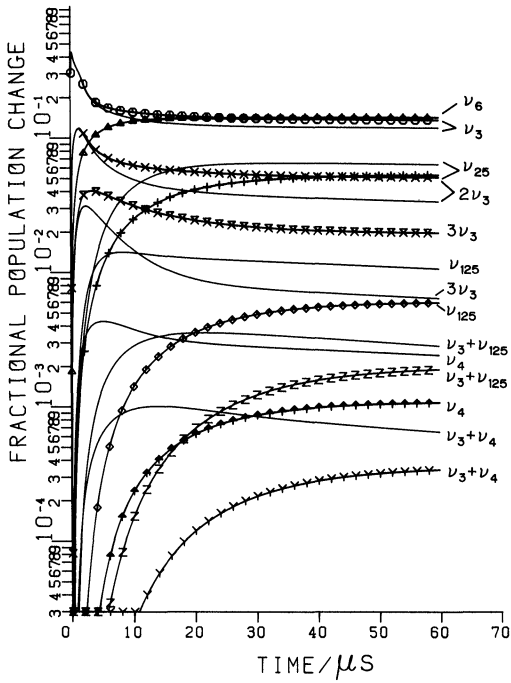

Figure 10 (c) Calculated fractional population changes in respective levels of CH_3F irradiated with the CO_2 laser at the fluence of 1 J cm^{-2}. The curves marked with various symbols show the values calculated based on the kinetic scheme without the $3\nu_3 \longleftrightarrow \nu_4$ V–V energy transfer, while the curves without symbols show those based on the scheme without the above V–V energy transfer.

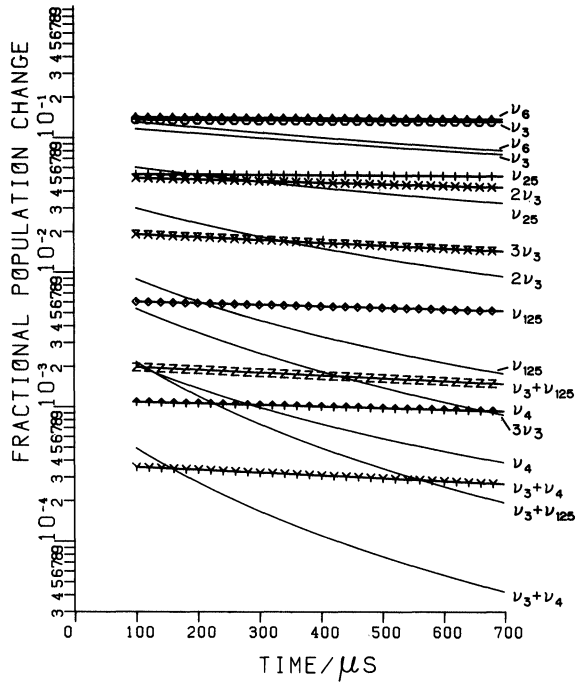

Figure 10 (d) Calculated results of (c) in the later stage of the relaxation.

population in the ν_4 level is accelerated greatly due to the direct energy flow from $3\nu_3$ just after the laser excitation to reach a maximum. Then, the ν_4 population is reduced due to the intermode V–V energy transfer to $\nu_1, 2\nu_5, \nu_2 + \nu_5$ and other nearby levels and also to ν_6, ν_2 and ν_5 modes *via* the $3\nu_3$ level since the excess energy accumulated in the ν_3 mode in the initial stage must be transferred to other levels. As already demonstrated in Figure 8, the observed emission data from ν_4 are in good agreement with the present model calculation.

Another significant finding in the kinetic model, including the $3\nu_3 \longleftrightarrow \nu_4$ V–V energy transfer, is that the vibrational quasiequilibrium population distribution may not be realized even in the final stage of the relaxation. In Figure 10(d), the population in each level decays in a non-exponential manner and the population ratio of certain levels is not constant during the course of the relaxation. On the contrary, in the case of weak laser excitation, as shown in Figure 10(b),

the population distribution in the respective levels is in equilibrium at a single vibrational temperature in the final stage of relaxation; populations in all levels decay with the same rate, the V–T/R rate. Referring to Figure 10(d), it is seen that the non-exponential population decay is more significant in higher levels, $\nu_3 + \nu_4$, $\nu_3 + \nu_{125}$, ν_4, $3\nu_3$, . . ., and the populations in lower levels are reduced almost exponentially although the rate is larger than the V–T/R rate.

This non-exponential population decay is caused by the existence of the $3\nu_3 \longleftrightarrow \nu_4$ V–V energy transfer. When this process is very efficient, a series of intermode V–V energy transfers occurs from $3\nu_3$ to $2\nu_3$ (see Figure 1) connecting levels which are located in between the two levels. This energy flow must occur if the relative population distribution in these levels exceeds the thermal one at room temperature, since the non-resonant energy of a V–V energy transfer process is transferred to/from translation and/or rotation whose energy distribution is in equilibrium at room temperature. After the successive intermode V–V energy transfers from the $3\nu_3$ to the $2\nu_3$ level, one quantum of the ν_3 vibration is transferred to translation and/or rotation. Further ν_3 quanta are lost if the intramode V–V pumping occurs within the ν_3 mode such as $2\nu_3 + \nu_3 \rightarrow 3\nu_3 + 0$. The overall process is that proposed by Mandich and Flynn[20] for the vibrational relaxation of N_2O and named a "catastrophic cyclic path". Since the cyclic path includes the intramode V–V energy transfer whose rate is a non-linear function with respect to the number density in a ν_3-excited level, the population decay in each relevant level must be dependent on the extent of the excitation and be non-exponential against time. The decay rate is much larger than that of the V–T/R energy transfer which is a linear process.

The Coriolis interaction of high rotational levels of the $3\nu_3$ level with those of the ν_4 level has been pointed out by Graner[4], who suggested an efficient energy transfer between $3\nu_3$ and ν_4 through Coriolis-coupled rotational levels. Later, his group carried out the intensive analysis of the high resolution spectrum in the 3-μm region, $\nu_4(E)$, $\nu_1(A)$, $2\nu_2(A)$, $2\nu_5(A_1 + E)$, $\nu_2 + \nu_5(E)$[5,6]. According to their analysis, $3\nu_3$, which lies $90\,cm^{-1}$ higher than ν_4, interacts with ν_4 leading to localized level crossing due to Coriolis coupling. Since the ν_2 and ν_5 fundamentals are only $8.4\,cm^{-1}$ apart, their overtone levels are coupled by a strong Coriolis interaction and, thus, the same Coriolis coupling must be significant in $2\nu_2$ with $\nu_2 + \nu_5$ and in $\nu_2 + \nu_5$ with $2\nu_5$. Furthermore, a

strong Fermi resonance is found in the ν_1 band since two parallel bands of equal intensity exist; the overtone level involved in the coupling is $2\nu_2$ or $2\nu_5$. The ν_4 band is relatively separate although a Fermi resonance between ν_4 and $2\nu_5$ must be taken into account. Thus, in the present kinetic model, only three levels, $3\nu_3$, ν_4 and ν_{125}, are introduced for the levels in the C—H stretching vibration region.

The conclusion derived in the former experiment[8,16] was criticized by Apkarian *et al.*[10] According to their numerical solution of rate equations, which are formulated for seven excited vibrational levels, ν_3, ν_6, ν_2/ν_5, $2\nu_3$, $2(\nu_2/\nu_5)$, ν_1/ν_4, and $3\nu_3$, under the initial condition of 40% CH_3F being in the ν_3 level and the remaining fraction in the ground level, the ν_1/ν_4 level is populated quickly to reach a peak, while $2(\nu_2/\nu_5)$ is not, even if the $3\nu_3 \longleftrightarrow \nu_1/\nu_4$ direct V–V energy transfer is included in the kinetic scheme. They attributed this to a small vibrational heat capacity of the $3\nu_3$ level relative to that of the ν_1/ν_4 and $2(\nu_2/\nu_5)$ levels, and suggested that a pathway from $2\nu_3$ to $2(\nu_2/\nu_5)$ *via* $\nu_x(\nu_3 + \nu_6, 2\nu_6, \nu_3 + \nu_2/\nu_5$, etc.) contributed significantly to the population of the levels in the C—H stretching region. Their calculation was extended to the CH_3F/Ar mixture, in which we demonstrated very efficient excitation of ν_4, ν_1 and other nearby levels in strong laser excitation[16], and claimed that their model could not reproduce the rapid accumulation of population in these levels. Thus, they concluded that the $3\nu_3 \longleftrightarrow \nu_4$ direct V–V energy transfer could not contribute largely to the entire relaxation in strong laser excitation of CH_3F at a low pressure (0.5 Torr) or in a mixture with Ar at a higher pressure (70 Torr).

The present kinetic model is essentially similar to the one adopted by Apkarian *et al.*[10], although seven excited levels in their model are replaced by 14 levels which include ν_x in their notation. The rate equations describing the initial stimulation processes are not included in their model, but, instead, an initial excitation condition is assumed which is almost in accord with the present average number of photons absorbed at a fluence of 0.5 J cm^{-2} (see Figure 6). The only essential difference in the present calculation from that of Apkarian *et al.* is that their adopted rate constant for the $\nu_1/\nu_4 \longleftrightarrow 2(\nu_2/\nu_5)$ V–V energy transfer is much smaller than that for the $\nu_4 \longleftrightarrow \nu_{125}$ given in Table III. However, this value is possibly larger than those accepted normally because of a very strong interaction between the relevant levels that has been proved by high resolution IR spectroscopy[5,6]. For the kinetic

calculation in the CH_3F/Ar mixture, Apkarian *et al.* assumed the absorbed photon number per CH_3F molecule to be 0.40 or 0.44. However, this number has been measured to be as large as 6 in the mixture of 0.12 Torr CH_3F and 120 Torr Ar at the laser fluence of $1\,J\,cm^{-2}$. Therefore, the assumed extent of their excitation is very much underestimated, and may not be the basis for discussion of the role of the $3\nu_3 \longleftrightarrow \nu_4$ V–V energy transfer in the relaxation. For the excitation and relaxation kinetics of CH_3F or other molecules in a dense third body medium will be reported elsewhere.

In the present kinetic calculation simulating the experimental data, it has been concluded that a cyclic series of the V–V energy transfers $2\nu_3 \longleftrightarrow \nu_x \longleftrightarrow 2\nu_5/\nu_2 + \nu_5/2\nu_2/\nu_1 \longleftrightarrow \nu_4 \longleftrightarrow 3\nu_3 \longleftrightarrow 2\nu_3$ plays a significant role in the relaxation of CH_3F whose ν_3 mode is highly excited. The conclusion derived by Apkarian *et al.*[10] that the $3\nu_3$ level may not contribute significantly to the filling of $2(\nu_2/\nu_5)$ in either the low or high excitation regime is not consistent with the present finding of non-exponential decay of populations in higher vibrational levels in the final stage of relaxation. As shown in Figure 10(c) and (d), this phenomenon could not be explained by the mechanism without the $3\nu_3 \longleftrightarrow \nu_4$ V–V energy transfer process.

The non-linear type relaxation found in the present experiment was also reported in the LIF kinetic studies[21] of COF_2 whose ν_2 mode is excited by an intense CO_2 laser. In weak laser excitation of COF_2, which was carried out by Castleton and Flynn[22], the LIF at 5 μm rose rapidly by the $\nu_2 \longleftrightarrow 2\nu_2$ intramode ladder climbing to reach a peak, which decayed biexponentially; the fast decay was assigned to V–V energy transfers from ν_1, ν_2 to the other modes, while the final decay was due to the V–T/R process. Contrary to this, in strong laser excitation, the 5-μm LIF of the final stage of the relaxation decayed non-exponentially; the rate defined from the decay slope became smaller in the later stage of relaxation. This observation is common to the present finding on ν_3-excited CH_3F by the TEA CO_2 laser, and might be caused by a mechanism similar to that proposed in this experiment.

Dependence on laser fluence

In the experiment of Sheorey and Flynn[2], CH_3F was excited by a Q-switched CO_2 laser with energy of about 1 mJ, and the induced 3-μm

emission was found to increase almost exponentially after the laser pulse (*see* Figure 6(b) of Ref. 2). This observation is consistent with the energy flow pathway in Eqn (1): $\nu_3 \rightarrow \nu_6 \rightarrow \nu_2/\nu_5 \rightarrow 2(\nu_2/\nu_5) \rightarrow \nu_1 \rightarrow \nu_4$. The present experiment of strong laser excitation indicates that the mechanism in Eqn (1) must be supplemented by taking into consideration the intermode V–V energy transfers such as $3\nu_3 \longleftrightarrow \nu_4$. The kinetic model thus postulated should be applicable to more general cases in the wide range of the extent of laser excitation.

In order to test the applicability of the present kinetic model, the 3-μm LIF was observed as a function of the laser fluence and compared with kinetic calculations. As shown in Figure 11, at the laser fluence of

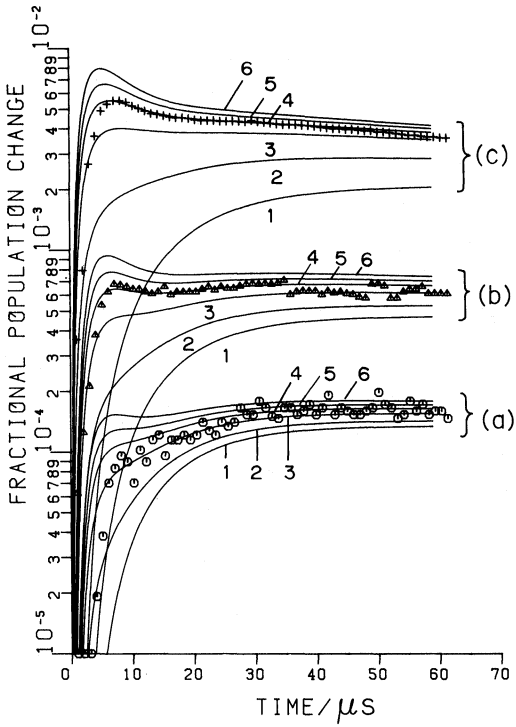

Figure 11 Observed and calculated time-evolved 3-μm emissions in CH_3F at 0.5 Torr as a function of the laser fluence together with the results calculated based on the scheme given in Table III with the rate constant of the $3\nu_3 \longleftrightarrow \nu_4$ V–V energy transfer of 0(1), 1×10^5(2), 3×10^5(3), 5×10^5(4), 7×10^5(5) and 1×10^6 s^{-1} $Torr^{-1}$(6). The laser fluence is 0.011(a), 0.04(b) and 0.46 J cm^{-2}(c).

$0.46\,J\,cm^{-2}$, the emission intensity increased rapidly to form a peak in the initial stage, while at $0.011\,J\,cm^{-2}$ its increase is much slower showing an exponential growth. The numerical solutions of the kinetic Eqns (16), (21–34) are also presented. The calculation was made by use of the rate constants listed in Table III except $k_{333,4}$, several values of which were assumed to optimize the simulation. The relative intensities of the 3-μm emission are given as a sum of populations in ν_4, ν_1 and other relevant levels with weights which are taken from relative absorption band intensities[14].

As pointed out previously, in the mechanism without the $3\nu_3 \longleftrightarrow \nu_4$ V–V energy transfer, the 3-μm emission intensity increases after an induction period which is almost independent of the laser fluence. Thus, to simulate the dependence of the 3-μm emission intensity on the laser fluence, it is inevitable to introduce the $3\nu_3 \longleftrightarrow \nu_4$ V–V energy transfer in the mechanism. If the value of $k_{333,4}$ is assumed to be $5 \times 10^5\,s^{-1}\,Torr^{-1}$, the present kinetic model may reproduce the observed 3-μm emission of CH_3F laser excited with the fluence in the range of 0.01–0.5 J cm^2.

CONCLUSION

When CH_3F is excited in its ν_3 mode by irradiation with an intense CO_2 laser pulse, the energy flow pathway from ν_3 to ν_4, ν_1 and other nearby levels has been proved to be the pathway in Eqn (1) combined with that in Eqn (2); the former is generally accepted in weak laser excitation,

$$\nu_3 \rightarrow \nu_6 \rightarrow \nu_2,\ \nu_5 \rightarrow 2\nu_5,\ \nu_2 + \nu_5,\ 2\nu_2 \rightarrow \nu_1 \rightarrow \nu_4 \qquad (1)$$

and the latter involves the intermode V–V energy transfer from the high overtone level, $3\nu_3$ to ν_4, which is Coriolis coupled:

$$\nu_3 \rightarrow 2\nu_3 \rightarrow 3\nu_3 \rightarrow \nu_4 \rightarrow \nu_1 \rightarrow 2\nu_2,\ \nu_2 + \nu_5,\ 2\nu_5 \qquad (2)$$

The relaxation mechanism of CH_3F in strong laser excitation is characterized by the above intermode V–V energy transfer.

In the initial stage of the relaxation of ν_3-excited CH_3F by strong laser irradiation, ν_4, ν_1 and other nearby levels are populated rapidly to reach a peak, which decays to a second broad maximum or to a plateau depending on the excitation condition. In the final stage of the relaxation, a quasiequilibrium vibrational distribution may not be

established, since a non-linear type relaxation, which is composed of the successive V–V energy transfers from $3\nu_3$ to $2\nu_3$ through ν_4, ν_1, and other closely lying levels, is much more efficient for transferring the vibrational energy to the translation and/or rotation than the V–T/R energy transfer from modes having low vibrational frequencies.

The present kinetic mechanism of non-linear type relaxation could be generalized for the intermode vibrational energy flow of polyatomic molecules whose single mode is excited by strong laser irradiation. Intermode V–V energy transfers from high overtone levels of a laser-excited mode to singly excited levels of other modes play a significant role in causing non-linear relaxation kinetics which are quite different from those normally accepted under low excitation conditions.

Acknowledgement

The authors thank Professor S. R. Leone for his critical reading of the manuscript.

References

1. G. W. Flynn, *Acc. Chem. Res.* **14**, 334 (1981); G. W. Flynn and E. Weitz, *Adv. Chem. Phys.* **47**, 185 (1981).
2. R. S. Sheorey and G. W. Flynn, *J. Chem. Phys.* **72**, 1175 (1980).
3. V. A. Apkarian and E. Weitz, *J. Chem. Phys.* **71**, 4349 (1979).
4. G. Graner, *J. Phys. Chem.* **83**, 1491 (1979).
5. G. Graner and G. Guelachvili, *J. Mol. Spectrosc.* **89**, 19 (1981).
6. J. P. Champion, A. G. Robiette, I. M. Mills and G. Graner, *J. Mol. Spectrosc.* **96**, 422 (1982).
7. M. Kneba and J. Wolfrum, *Ber. Bunsenges. Phys. Chem.* **81**, 1275 (1982).
8. H. Nakane and S. Tsuchiya, *Chem. Phys. Lett.* **80**, 458 (1981).
9. R. A. Forber, R. E. McNair, S. F. Fulghum, M. S. Feld and B. J. Feldman, *J. Chem. Phys.* **72**, 4693 (1980).
10. V. A. Apkarian, J. M. Lindquist and E. Weitz, *Chem. Phys. Lett.* **112**, 328 (1984).
11. T. J. Manuccia and D. S. Frankel, *Rev. Sci. Instr.* **49**, 337 (1978).
12. H. L. Welsh, E. J. Stansburgh, J. Romanko and T. Feldman, *J. Opt. Soc. Am.* **45**, 338 (1955).
13. T. Y. Chang, *Opt. Commun.* **2**, 77 (1970).
14. J. Gigure and J. Overend, *Spectrochim. Acta* **32A**, 241 (1976).
15. A. D. Devir and U. P. Oppenheim, *J. Chem. Phys.* **67**, 691 (1977).
16. H. Nakane and S. Tsuchiya, *Chem. Phys. Lett.* **84**, 322 (1981).
17. S. Saeki, M. Mizuno and S. Kondo, *Spectrochim. Acta* **32A**, 403 (1976).
18. S. M. Freund, G. Duxbury, M. Roheld, J. T. Tiedjo and T. Oka, *J. Mol. Spectrosc.* **52**, 38 (1974).
19. T. Shimanouchi, Table of Molecular Vibrational Frequencies, NSRDS-NBS 39 (US Government Printing Office, Washington, DC, 1972).
20. M. L. Mandich and G. W. Flynn, *J. Chem. Phys.* **73**, 3679 (1980).
21. A. Karbach, C. Sayer and P. Hess, *Chem. Phys.* **96**, 461 (1985).
22. K. H. Castleton and G. W. Flynn, *J. Chem. Phys.* **67**, 3133 (1977).
23. E. Weitz and G. W. Flynn, *J. Chem. Phys.* **58**, 2781 (1973).